

## Determination of relaxation time of a Josephson junction qubit

S. K. Dutta, H. Xu, A. J. Berkley, R. C. Ramos, M. A. Gubrud, J. R. Anderson, C. J. Lobb, and F. C. Wellstood  
*Center for Superconductivity Research, Department of Physics, University of Maryland, College Park, Maryland 20742-4111, USA*  
 (Received 16 May 2004; published 7 October 2004)

When a Josephson junction in the zero-voltage state is current-biased below its critical current, the rate that it escapes to the finite-voltage state depends on the quantum state of the junction. By employing a slow current sweep, it is possible to observe experimentally the emptying of the thermally populated first excited level as a well-defined feature in the escape rate. This feature provides a simple method of determining the junction's energy relaxation time  $T_1$ , a key parameter for evaluating its utility for quantum computation. We discuss the temperature regime where this effect is readily observable and describe how the emptying depends directly on the relaxation time. Our model of the junction dynamics agrees well with the measured escape rate of a  $10\ \mu\text{m} \times 10\ \mu\text{m}$  Nb-AlOx-Nb device in the 25 to 300 mK temperature range, yielding  $T_1 \approx 4$  ns.

DOI: 10.1103/PhysRevB.70.140502

PACS number(s): 74.50.+r, 03.67.Lx, 85.25.Cp

Over the last two decades, observations of macroscopic quantum tunneling<sup>1</sup> and energy level quantization<sup>2</sup> have established the importance of quantum phenomena in single current-biased Josephson junctions. Recent interest in these devices stems from the proposal that they be used as qubits for quantum computation.<sup>3</sup> The observation of Rabi oscillations<sup>4,5</sup> and evidence for entangled states in coupled junctions<sup>6</sup> have lent some substance to this approach. However, a key issue is that these superconducting qubits must be attached to bias leads. This direct coupling to a dissipative environment gives rise to both interlevel transitions (on a time scale of the relaxation time  $T_1$ ) and destruction of phase coherence in quantum states (with scale of the coherence time  $T_2$ ). While the coherence time sets the limit on the number of consecutive gate operations that could potentially be performed, the relaxation time serves as an upper bound on  $T_2$  and is an important measure of the isolation of the qubit. Accurate measurements of  $T_1$  could better characterize the system, possibly revealing the source of the wide range of single junction  $T_2$ 's recently reported in the literature.<sup>4,5,7</sup>

It is not easy to determine the relaxation time reliably in the single junction system. For example, it is difficult to predict  $T_1$  based solely on the circuit wiring design because the circuit parameters must be accurately known at high frequencies. Additional sources of dissipation, such as quasiparticles,<sup>8</sup> further complicate the situation. Several techniques for measuring  $T_1$  have been demonstrated, but proper execution of these methods tends to be technically challenging. It is, for example, possible to excite the junction with a microwave pulse and measure the decay time back to its ground state.<sup>5</sup> However, if a resonance of the apparatus is also excited, the resulting decay may be determined by the lifetime of the resonance, rather than that of the junction. Similarly, the junction can be excited by a "dc pulse" in the bias current,<sup>9</sup> but the bandwidth of the bias and detection lines must be sufficiently high so as not to influence the results. Care must also be taken that this extra bandwidth does not introduce additional noise. Alternatively, by ramping the bias current quickly, the population of thermally excited states is in effect frozen, and the emptying of each level can be seen quite dramatically in the escape rate.<sup>10</sup> A drawback of this fast ramp technique is that it requires a very

accurate calibration of the current ramp to extract  $T_1$  from the data. A related approach makes use of a slow sweep, which gives features dependent on the junction shunting resistance  $R$ , while the system maintains dynamic equilibrium at elevated temperature.<sup>11</sup> However, determining this resistance from either the slow or fast sweep will in general require detailed modeling and knowledge of the system,<sup>12</sup> especially when the junction temperature is much higher than its characteristic frequency, as the escape rate may depend strongly on parameters aside from  $R$ .

In this paper, we show how a nearly stationary bias sweep, with a careful choice of the junction temperature and sweep rate, can be used to identify  $T_1$  directly. With this method, which is easy to implement and does not require the use of microwave activation, an estimate of  $T_1$  can be obtained with straightforward analysis.

The system is modeled as an idealized Josephson junction [see Fig. 1(a)] shunted by a capacitor  $C$  and a frequency-

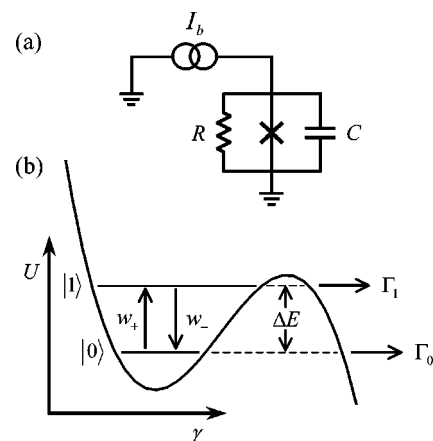


FIG. 1. (a) Schematic diagram of a current-biased Josephson junction, with effective shunting resistance  $R$  and capacitance  $C$ . (b) Tilted washboard potential  $U(\gamma)$  with two energy levels separated by  $\Delta E$ . The system can tunnel to the voltage state from the ground state and first excited state with rates  $\Gamma_0$  and  $\Gamma_1$ , respectively. Interlevel transitions with rates  $w_+$  and  $w_- \approx 1/T_1 \approx 1/RC$  keep the system in thermal equilibrium, in the absence of tunneling.

independent resistance  $R$ . This resistance is the inverse of the real part of the shunting admittance, evaluated at the plasma frequency of the junction, and is assumed to be responsible for all dissipation in the system. The dynamics of the system are analogous to a particle with coordinate  $\gamma$  and mass  $C(\Phi_0/2\pi)^2$ , moving in a tilted washboard potential<sup>13</sup>

$$U(\gamma) = -\frac{\Phi_0}{2\pi}(I_c \cos \gamma + I_b \gamma), \quad (1)$$

where  $\gamma$  is the gauge-invariant phase difference across the junction,  $\Phi_0$  is the flux quantum,  $I_c$  is the critical current of the junction, and  $I_b$  is the bias current through it.

For  $I_b < I_c$ , this potential defines metastable quantum states, which describe the zero-voltage state of the junction [see Fig. 1(b)]. If the junction temperature is low enough, only the two lowest states have a non-negligible probability of being occupied. This simple situation will be discussed in some detail, as it is a valuable one for extracting  $T_1$ . At temperature  $T$ , thermal excitations from the ground state  $|0\rangle$  to the first excited state  $|1\rangle$  occur at a rate<sup>14,15</sup>

$$w_+ = \frac{\Delta E}{2e^2 R} \frac{| \langle 0 | \gamma | 1 \rangle |^2}{e^{\Delta E/k_B T} - 1}, \quad (2)$$

where  $\Delta E$  is the energy level spacing between the two levels. From detailed balance, transitions from  $|1\rangle$  to  $|0\rangle$  must occur at a rate

$$w_- = w_+ e^{\Delta E/k_B T} \approx \frac{1}{RC} + w_+, \quad (3)$$

where the approximation assumes harmonic oscillator-like states (valid provided  $I_b$  is not too close to  $I_c$ ). The first term, which dominates at low temperature, can be attributed solely to relaxation, so that  $T_1 \approx RC \approx 1/w_-$ . In addition to the interlevel transitions, the states  $|0\rangle$  and  $|1\rangle$  can tunnel to the finite-voltage continuum of states with rates  $\Gamma_0$  and  $\Gamma_1$ , respectively.

To understand our technique for determining  $T_1$ , consider a junction that is allowed to evolve with these four transition rates ( $w_+, w_-, \Gamma_0, \Gamma_1$ ) while  $I_b$  is linearly ramped with time. The ramp begins at  $t=0$ , with  $I_b=0$  and the junction in the zero-voltage state. The sweep proceeds slowly enough for the system to stay in dynamic equilibrium at all times, until the junction switches to the voltage state. In the noncoherent limit (i.e., on a time scale longer than  $T_2$ ), the evolution of the system can be described by a master equation<sup>14,15</sup>

$$\frac{\partial \rho_0}{\partial t} = (-\Gamma_0 - w_+) \rho_0 + w_- \rho_1, \quad (4a)$$

$$\frac{\partial \rho_1}{\partial t} = w_+ \rho_0 + (-\Gamma_1 - w_-) \rho_1, \quad (4b)$$

where  $\rho_0(t)$  and  $\rho_1(t)$  are the probabilities that the system is in  $|0\rangle$  and  $|1\rangle$  at time  $t$ . Here, the four transition rates are functions of  $I_b$ , which itself varies with  $t$ . The probability  $\rho(t) = \rho_0(t) + \rho_1(t)$  that the junction is in the zero-voltage state decreases with time, due to escape to the finite-voltage state.

It is convenient to introduce the conditional probabilities

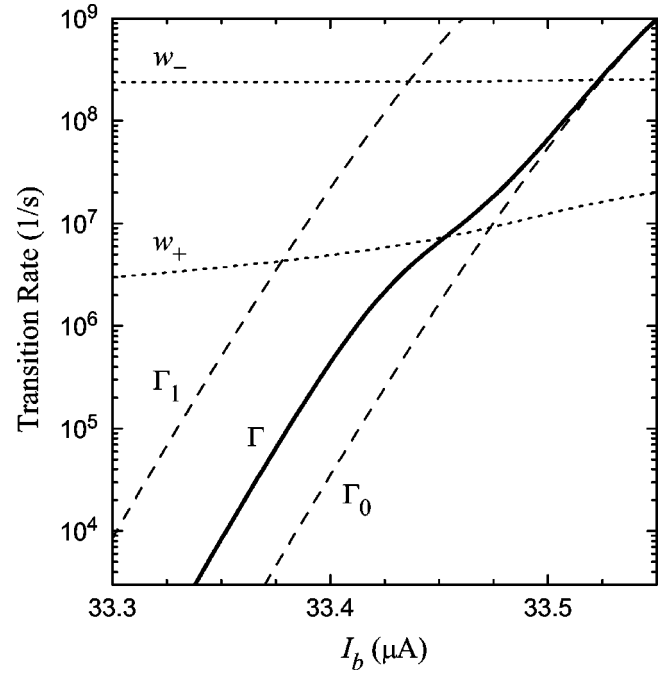


FIG. 2. Theoretical values for the tunneling (dashed lines) and interlevel transition (dotted) rates for a two-level system, for a junction with critical current  $I_c=33.65 \mu\text{A}$ , relaxation time  $T_1=4.2 \text{ ns}$ , at temperature  $T=98 \text{ mK}$ . The total escape rate  $\Gamma$  (solid) [calculated with Eqs. (6) and (7)] collapses to  $\Gamma_0$  as the excited state population vanishes under a stationary current sweep, i.e.,  $\Gamma$  has no implicit time dependence. Emptying occurs at the bias current where  $\Gamma_1 \approx w_-$ , resulting in a feature at  $\Gamma \approx \Gamma_0 + (1/2)w_+$ .

$$P_0 \equiv \rho_0/\rho, \quad P_1 \equiv \rho_1/\rho, \quad (5)$$

which give the probabilities that a junction which has yet to escape is in  $|0\rangle$  and  $|1\rangle$ , respectively. Note that  $P(t) \equiv P_0(t) + P_1(t) = 1$  for all time. The rate that the system escapes to the voltage state (an experimentally accessible quantity) from both states is given by

$$\Gamma = -\frac{1}{\rho} \frac{d\rho}{dt} = \Gamma_0 P_0 + \Gamma_1 P_1. \quad (6)$$

$\Gamma_0$  and  $\Gamma_1$  increase exponentially with  $I_b$ . If  $I_b$  increases linearly with time, then the escape rates will increase exponentially with time as well. For the moment, let their time dependence be given by  $e^{\alpha t}$ . It can be shown that  $\partial P_0/\partial t$  and  $\partial P_1/\partial t$  are negligible when the bias current is changing slowly enough so that  $\alpha \ll w_-$ . In this stationary limit, Eqs. (4) and (5) give

$$\frac{P_1}{P_0} = \frac{-(\delta w + \delta \Gamma) + \sqrt{(\delta w + \delta \Gamma)^2 + 4w_+ w_-}}{2w_-}, \quad (7)$$

where  $\delta w \equiv w_- - w_+$  and  $\delta \Gamma \equiv \Gamma_1 - \Gamma_0$ .

Equation (7) reveals that at low temperatures, where  $w_- \gg w_+$ ,  $P_0 \approx 1$  for all bias currents, while  $P_1 \approx w_+/(w_- + \delta \Gamma)$ . This excited state occupation probability is qualitatively different for high and low values of  $I_b$ . At low bias currents, where  $\Gamma_1 \ll w_-$ , the system is essentially in thermal equilibrium because tunneling is negligible. In this limit, the total

escape rate reduces to  $\Gamma = \Gamma_0 + \Gamma_1 e^{-\Delta E/k_B T}$ . In contrast, at high currents,  $\Gamma_1 \gg w_- \gg w_+$ , so that  $P_1$  vanishes and  $\Gamma$  collapses to  $\Gamma_0$ . This implies that the first excited state is highly depopulated as a result of strong tunneling from this state. As shown in Fig. 2 [generated with Eqs. (6) and (7)], the shift between these two limiting behaviors occurs near the bias current (denote it  $I_b^*$ ) where  $\Gamma_1 = w_-$ . Note that  $I_b^*$  is only weakly dependent on temperature through  $w_-$ . The corresponding total escape rate at the crossing point is  $\Gamma \approx \Gamma_0 + \frac{1}{2}w_+$ , using the fact that  $\Gamma_1 \gg \Gamma_0$ .

$\Gamma_0$  increases with  $I_b$  much more quickly than  $w_+$  does, resulting in a clear shoulder feature in  $\Gamma$  at the crossover. Therefore  $w_+$  and  $I_b^*$  may be estimated directly from the total escape rate curve without any fitting, simply by identifying the location of this feature. If  $T$  and  $\Delta E(I_b^*)$  are known (from spectroscopic measurements, for example), then  $T_1$  can be estimated as  $e^{-\Delta E/k_B T}/w_+$ . Once again, however, an approximate value can be found from escape rate curves.  $\Gamma_0(I_b)$  may be found by measuring the total escape rate at very low temperature, where  $P_1$  is not just small, but negligible at all values of the bias current. While  $\Gamma_1/\Gamma_0$  is a function of  $I_b$ , our simulations suggest that this ratio, evaluated at  $I_b^*$ , is on the order of 500 for a large range of  $T_1$ , thus

$$T_1 \approx [500 \Gamma_0(I_b^*)]^{-1}. \quad (8)$$

At sufficiently high temperatures, levels above the first excited state will have a finite occupation probability. Each of the levels will empty out in order, leading to a series of shifts in  $\Gamma$ , as opposed to a single distinct feature. Such features have been previously reported for a range of bias sweep rates.<sup>11</sup>

Experiments to measure  $T_1$  were performed on a  $10 \mu\text{m} \times 10 \mu\text{m}$  Nb-AlOx-Nb thin film trilayer Josephson junction with a  $100 \text{ A/cm}^2$  critical current density, fabricated by Hypres, Inc.<sup>16</sup> The device was mounted on the mixing chamber of an Oxford Instruments dilution refrigerator. The bias current lines were filtered using homemade rf and microwave powder filters, and an additional on-chip LC filter (with a 200 MHz resonance frequency) was used to further isolate the junction from the environment.<sup>17</sup> An external magnetic field, of a few millitesla in the plane of the junction, was used to tune  $I_c$  to roughly  $30 \mu\text{A}$ , where  $\Delta E/h \approx 6 \text{ GHz}$  for bias currents of interest.

To determine the escape rate  $\Gamma$ ,  $I_b$  was ramped from zero to  $I_c$  at a fixed rate. We measured the time between the start of the ramp and the detection of a voltage across the junction, signifying tunneling out of the zero-voltage state, and converted the time into the bias current at which the switch occurred. This procedure was repeated  $10^5$  times at a fixed mixing chamber temperature to get a histogram of switching events, from which  $\Gamma$  was calculated.<sup>18</sup>

Figure 3 shows  $\Gamma$  as a function of  $I_b$  for a ramp rate of  $0.9 \text{ A/s}$ , at temperatures between 25 and 310 mK. At the lowest temperature, the escape rate is roughly exponential in the bias current, as expected for tunneling out of the ground state alone. As the junction temperature is increased, thermal excitations populate higher energy levels, leading to higher escape rates at low  $I_b$ . As discussed above, these excited levels will depopulate as  $I_b$  is swept to  $I_c$ . Eventually, only

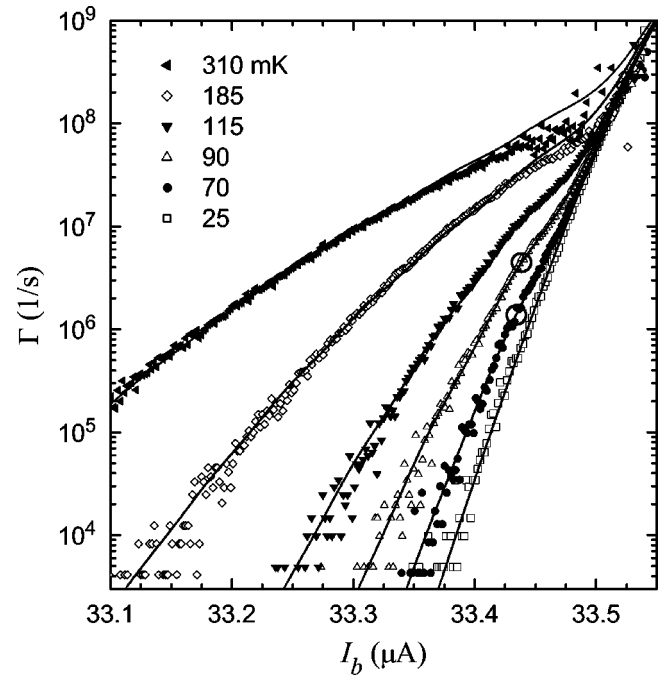


FIG. 3. Total escape rate  $\Gamma$  of an Nb-AlOx-Nb Josephson junction at six temperatures (symbols), taken with a bias current sweep rate of  $0.9 \text{ A/s}$ . The two large open circles indicate the location of the feature that can be used to estimate  $T_1$ . Solid lines show the result of master equation simulations with  $R=1\text{k}\Omega$  and  $C=4.2 \text{ pF}$ .

escapes from the ground state are observed, so that all of the curves collapse onto each other at high  $I_b$ . The data show that the  $\Gamma$  corresponding to this convergence increases with temperature, due to the concurrent increase of  $w_+$ .

The ramp rate was chosen to be just high enough to follow the described trend. At lower rates, too much time is spent at low  $\Gamma$ , so that the junction almost always escapes before the collapse. At higher rates, the sweep goes further into the nonstationary regime, where it influences  $\Gamma$ , unnecessarily complicating matters. However, even at the selected rate (where the sweep rate parameter  $\alpha$  is  $7 \times 10^7 \text{ 1/s}$ ), some adjustments were made to the calibration of  $I_b$  with respect to time. In correcting the calibration, we compared the base temperature escape rate curve taken at  $0.9 \text{ A/s}$  with data taken at a slower sweep rate ( $0.07 \text{ A/s}$ ), where the calibration could be performed more accurately. In addition, a small offset was added to  $I_b$  for each temperature, to reproduce the expected coincidence of the curves at high escape rates. These adjustments, all less than  $15 \text{ nA}$ , could be needed due to an incomplete knowledge of the calibration (e.g., its temperature dependence), or to small drifts in the detection electronics or junction critical current over the course of the data taking.

At 70 and 90 mK, there is a relatively small deviation in  $\Gamma$  from its base temperature values, suggesting that the above two-level analysis can be applied to these data. The existence of a single well-defined shoulder supports this claim. Using Fig. 2 as a guide, this feature begins at  $I_b \approx 33.435 \mu\text{A}$ , as indicated by large open circles in Fig. 3. At this current, we can read off  $\Gamma_0(I_b^*) \approx 5 \times 10^5 \text{ 1/s}$  and thus our rough rule Eq. (8) gives  $T_1 \approx 4 \text{ ns}$ .

To perform a more quantitative analysis of the data, we computed tunneling rates, interlevel transition rates, and the spacing of energy levels, by solving the time-independent Schrödinger equation on a grid, using transmission boundary conditions at the edge of the potential well. Fitting to the base-temperature escape rate (which is almost independent of  $R$ ,  $T$ , and sweep rate) gives  $I_c=33.65 \mu\text{A}$  and  $C=4.2 \text{ pF}$ . To fit the higher temperature curves, the master equation for eight energy levels<sup>14,15</sup> and a  $0.9 \text{ A/s}$  sweep rate is used (solid lines in Fig. 3). The effective resistance  $R$  was held at a constant value of  $1 \text{ k}\Omega$  for all of the fits, yielding  $T_1 \approx 4 \text{ ns}$ , consistent with our rough estimate. For mixing chamber temperatures of  $70, 90, 115, 185,$  and  $310 \text{ mK}$ , the fit temperatures were  $73, 98, 134, 215,$  and  $340 \text{ mK}$ , respectively.

We note that all of the data are fit with single values of  $I_c$ ,  $R$ , and  $C$ , and that the fits reproduce most features of the data. The discrepancy between the measured and fit temperatures, however, is of some concern. Also, while the emptying of  $|1\rangle$  matches well with theory, some subtle features of the higher levels are not entirely captured. These issues could be a result of failing to include higher order interlevel transi-

tions, neglecting the temperature dependence of  $R$ , making the simplification  $T_1=RC$ , or effects from the LC isolation.

In conclusion, slowly sweeping the bias current through a Josephson junction at moderately low temperature (roughly  $k_B T \approx \Delta E/3$ ) while measuring the total escape rate, provides a direct method for estimating the junction energy relaxation time  $T_1$ . This simple technique keeps the system near dynamic equilibrium and does not require the use of microwaves. High quality fits to the data give a value for the shunting resistance of the junction, demonstrating how the effectiveness of any junction isolation scheme can be readily evaluated. Finally, we note this technique can be used to independently confirm the large values for  $T_1$  in junction systems recently reported in the literature.

We thank K. C. Schwab and M. A. Manheimer for helpful discussions and R. A. Webb for experimental guidance, as well as for providing a critical vacuum pump when our own failed. This work has been funded by the National Security Agency, the National Science Foundation through the QUBIC program, and the Center for Superconductivity Research.

- 
- <sup>1</sup>R. F. Voss and R. A. Webb, Phys. Rev. Lett. **47**, 265 (1981).  
<sup>2</sup>J. M. Martinis, M. H. Devoret, and J. Clarke, Phys. Rev. Lett. **55**, 1543 (1985).  
<sup>3</sup>R. C. Ramos, M. A. Gubrud, A. J. Berkley, J. R. Anderson, C. J. Lobb, and F. C. Wellstood, IEEE Trans. Appl. Supercond. **11**, 998 (2001).  
<sup>4</sup>Y. Yu, S. Han, X. Chu, S. Chu, and Z. Wang, Science **296**, 889 (2002).  
<sup>5</sup>J. M. Martinis, S. Nam, J. Aumentado, and C. Urbina, Phys. Rev. Lett. **89**, 117901 (2002).  
<sup>6</sup>A. J. Berkley, H. Xu, R. C. Ramos, M. A. Gubrud, F. W. Strauch, P. R. Johnson, J. R. Anderson, A. J. Dragt, C. J. Lobb, and F. C. Wellstood, Science **300**, 1548 (2003).  
<sup>7</sup>A. J. Berkley, H. Xu, M. A. Gubrud, R. C. Ramos, J. R. Anderson, C. J. Lobb, and F. C. Wellstood, Phys. Rev. B **68**, 060502(R) (2003).  
<sup>8</sup>K. M. Lang, S. Nam, J. Aumentado, C. Urbina, and J. M. Martinis, IEEE Trans. Appl. Supercond. **13**, 989 (2003).  
<sup>9</sup>S. Han, Y. Yu, X. Chu, S. Chu, and Z. Wang, Science **293**, 1457 (2001).  
<sup>10</sup>P. Silvestrini, V. G. Palmieri, B. Ruggiero, and M. Russo, Phys. Rev. Lett. **79**, 3046 (1997).  
<sup>11</sup>B. Ruggiero, M. G. Castellano, G. Torrioli, C. Cosmelli, F. Chiarello, V. G. Palmieri, C. Granata, and P. Silvestrini, Phys. Rev. B **59**, 177 (1999).  
<sup>12</sup>C. Cosmelli, P. Carelli, M. G. Castellano, F. Chiarello, G. Diambrini Palazzi, R. Leoni, and G. Torrioli, Phys. Rev. Lett. **82**, 5357 (1999); S. Han and R. Rouse, *ibid.* **86**, 4191 (2001).  
<sup>13</sup>See, e.g., M. Tinkham, *Introduction to Superconductivity*, 2nd. ed. (McGraw-Hill, New York, 1996).  
<sup>14</sup>A. I. Larkin and Yu. N. Ovchinnikov, Zh. Eksp. Teor. Fiz. **91**, 318 (1986) [Sov. Phys. JETP **64**, 185 (1986)].  
<sup>15</sup>K. S. Chow, D. A. Browne, and V. Ambegaokar, Phys. Rev. B **37**, 1624 (1988).  
<sup>16</sup>The junction was capacitively coupled to an identical junction, for use in two-qubit studies. This extra junction was kept out of resonance with the experimental junction for the duration of the present work, by fixing its bias current to zero, so that  $\Delta E/h > 20 \text{ GHz}$ .  
<sup>17</sup>A. J. Berkley, H. Xu, M. A. Gubrud, R. C. Ramos, J. R. Anderson, C. J. Lobb, and F. C. Wellstood, IEEE Trans. Appl. Supercond. **13**, 952 (2003).  
<sup>18</sup>T. A. Fulton and L. N. Dunkleberger, Phys. Rev. B **9**, 4760 (1974).